HHS Public Access

Author manuscript

Int J Radiat Oncol Biol Phys. Author manuscript; available in PMC 2019 June 27.

Published in final edited form as:

Int J Radiat Oncol Biol Phys. 2019 January 01; 103(1): 268–275. doi:10.1016/j.ijrobp.2018.08.021.

The clinical and dosimetric impact of real-time target tracking in pancreatic SBRT

Yevgeniy Vinogradskiy, **Karyn A. Goodman**, **Tracey Schefter**, **Moyed Miften**, and **Bernard L. Jones**[a]

Department of Radiation Oncology, University of Colorado School of Medicine

Abstract

Purpose: Motion often hinders the safe delivery of ablative doses of radiation in the treatment of pancreatic tumors. Real-time tumor tracking methods are an emerging technique to increase the accuracy of delivery. In this study we report on a large, retrospective cohort of pancreatic patients treated with real-time, fiducial-based, kV image guidance of Stereotactic Body Radiotherapy (SBRT). The purpose of our study was to determine the impact of real-time tracking on treatment accuracy, tumor dose, and clinical workflow.

Methods: Real-time tracking data from 68 patients treated with pancreatic SBRT were analyzed. kV images orthogonal to the treatment beam were acquired in real-time during treatment to visualize the location of implanted fiducial markers. Positional corrections were made if the fiducial markers were observed >3 mm from the expected reference position. We recorded the frequency and nature of treatment interventions due to real-time tracking and derived a neural network-based dosimetric model to calculate the impact of these in-treatment interventions on target dose.

Results: Treatment pauses that required patient re-alignment due to real-time tumor tracking occurred during 32% of all fractions. The median magnitude of re-alignment shifts was 5.2 mm (range 2.1 – 18.9 mm). 45% of shifts resulted in dosimetric differences to the tumor; of these, the median point dose difference was 23% ± 22% of prescription dose (max 94%). The number of pauses per fraction was significantly higher in patients treated with respiratory gating (vs. abdominal compression) and in patients with greater treatment time.

Conclusions: Fiducial-based real-time target tracking is clinically feasible for pancreatic SBRT treatment. Our data indicate that real-time tumor tracking leads to patient re-alignment in 32% of cases and results in significant benefits to target coverage. The increased accuracy of real-time target tracking may potentially enable safe dose escalation in pancreatic SBRT.

I. INTRODUCTION

Stereotactic body radiation therapy (SBRT) is emerging as a promising treatment option for pancreatic tumors, especially in the treatment of locally advanced and/or borderline resectable disease (1, 2). Recent data has demonstrated that escalating dose to the pancreas can increase local control, but also increases the rate of gastro-intestinal toxicity (3). Given

a) Author to whom correspondence should be addressed: bernard.jones@ucdenver.edu.

the proximity of the pancreas to critical structures such as the duodenum and stomach, accurate delivery of focal ablative dose is paramount (4). However, the pancreas undergoes significant respiratory-induced motion which can decrease the accuracy of dose delivery (5).

The breathing-induced abdominal motion and the high delivery accuracy needed for SBRT requires motion management techniques to ensure safe treatment delivery. Traditional motion management approaches have involved the use of a 4-Dimensional Computed Tomography (4DCT). 4DCTs are used to assess the breathing-induced motion of the tumor (and surrounding organs) and aid with the motion management strategy during treatment. One can account for motion through the design of an Internal Target Volume (ITV) that encompasses the tumor range-of-motion (6–8). One can also reduce the amount of motion by either compressing the abdomen (2, 9) or gating the treatment beam during certain phase of the breathing cycle. However, these techniques often rely on data from 4DCTs, while recent studies have shown that due to the erratic motion of abdominal organs, a single 4DCT taken at simulation may not be adequate to describe the intrafraction motion of pancreatic tumors (10–15).

As a result of the inconsistent organ and tumor motion, using fiducial markers in conjunction with real-time image guidance has taken on an increased role in performing pancreas SBRT. Real-time intra-fraction target tracking has been developed to allow for direct measurement of the tumor location during treatment (10, 16–21). Tracking can be used in conjunction with other motion management techniques to identify periods of erratic breathing motion that can reduce the precision of the target localization during treatment. Fiducials are implanted in/around the tumor and, in addition to being used to help delineate the target, are used to align the patient for treatment and guide imaging throughout treatment to ensure that erratic motion has not caused the target to move out of the treatment volume (10, 12, 22–27).

As dose-escalated therapies become more commonplace in pancreatic SBRT, there is an even greater need for accurate delivery of dose through motion control. Since 2014, our institution has used in-treatment kV imaging for real-time target tracking of pancreatic tumors. The purpose of our study was to determine the clinical and dosimetric impact of real-time target tracking in pancreatic SBRT by answering three key clinical questions: what is the impact of real-time target tracking on 1) clinical workflow, 2) treatment accuracy, and 3) tumor dose? To answer these questions, we retrospectively analyzed data collected during pancreatic SBRT with real-time target tracking. These clinical data were used in conjunction with an artificial neural network-based dosimetric model to calculate the impact of real-time target tracking on tumor dose.

II. METHODS

A. Patient population and treatment characteristics

68 pancreatic cancer patients treated with SBRT using a fiducial-based real-time target tracking system were used for the study. All data was collected under an IRB-approved protocol for retrospective data analysis. A summary of major clinical and treatment characteristics of these patients is given in Table 1. Roughly one week prior to simulation, fiducial markers were inserted in or near the tumor using an ultrasound-guided endoscopic

probe by an experienced gastrointestinal surgeon. These markers were cylindrically-shaped (length 5 mm, width 1 mm) and composed of gold (Civco Radiotherapy, Orange City, IA). The most frequent number of implanted fiducials was 2 (26%) or 3 (54%).

For simulation and treatment, two motion management strategies were used: abdominal compression and amplitude-based (28–31) respiratory gating. The decision of whether to use abdominal compression or respiratory gating was made by the radiation oncologist. In general, preference was given to respiratory gating over compression because prior work has shown that gating results in lower average motion for pancreatic SBRT (with an average superior-inferior range of motion of 5.5 mm vs8.5 mm for compression) (32). Compression was used in cases where the patient was considered a poor candidate for gating due to compliance.

Abdominal compression was accomplished using an indexed, inflatable compression belt (Aktina Medical, Congers, NY). Belt pressure settings were determined by inflating the belt until the patient began to feel pain or discomfort. For patients treated with abdominal compression, a free-breathing CT scan with compression was used for treatment planning. Gating was accomplished using the Varian RPM system, and was delivered in the end-exhale phase using amplitude-based gating. In patients treated with gating, an end-exhale breath-hold CT was used for treatment planning. IV (iodine) and oral (barium) contrast were used to delineate nearby vessels and bowel, and a 4DCT was acquired to estimate tumor motion. The breath-hold and 4DCT was supervised using the Varian RPM system, and 4DCT images were sorted by phase. For patients managed with gating, patients received audio breathing instructions during the 4DCT where the frequency of the breathing period was pre-selected by the patient. All CTs were acquired with 3 mm slice thickness.

All treatment planning was done in Eclipse using Volumetric Arc Therapy (VMAT) (Varian Medical Systems, Palo Alto, CA). Gross tumor volumes (GTV) were drawn by the radiation oncologist on the planning CT, and expanded to create a Planning Target Volume (PTV). The GTV-to-PTV expansion margins were typically 3–5 mm, and were determined by the oncologist based on local anatomy. Our clinical workflow did not explicitly use an Internal Target Volume (ITV); motion was taken into account in the design of the PTV. The PTV contour was overlaid on the 4DCT, and compared against the observed range-of-motion. For patients managed with gating, the range-of-motion included the 30% to 70% phases of the 4DCT (end-exhale phases); whereas for patients managed with compression this motion included all phases. If needed, the PTV was expanded further to encompass this range-of-motion.

Prior to treatment, patient alignment was verified with fluoroscopy imaging (in the AP direction) and CBCT. For patients treated with abdominal compression, fluoroscopic images were acquired, and the fiducials aligned to the fiducial contours created during the planning process. A free-breathing CBCT was acquired and aligned to the planning CT using the fiducials as a guide. For patients treated with gating, patient alignment was first verified by fluoroscopic imaging taken during free breathing with the patient receiving the same audio coaching instruction that they received at simulation. Fluoroscopy also served to verify the appropriateness of the amplitude gating thresholds, since one can observe if the fiducials are

within the reference contours (defined in the following section) while the respiratory signal is within the gating thresholds (using the system's built-in color-coding scheme). The therapists were instructed to manually stop the fluoroscopic images at end-exhalation and align the captured image to the fiducials contoured on the breath-hold simulation CT. Finally, an end-exhale breath-hold CBCT was acquired, and the fiducial markers were used for localization. Since the time to acquire the CBCT (35 seconds) was longer than the typical length of time that patients can hold their breath at end-exhale (15 seconds), the CBCT was acquired over multiple breath holds (typically 2) if needed. Fluoroscopic images were acquired prior to CBCT images because fluoroscopy provides a complete picture of the motion of the fiducials and allows one to perform a couch longitudinal shift that aligns the markers exactly with the end-exhale position. Some patients have difficulty performing end-exhale breath hold, and this process allows one to detect if there are problems with the acquired CBCT.

B. Real-time target tracking workflow

Real-time tracking was implemented via kV imaging of implanted fiducial markers. In all cases, a reference position was determined that corresponded to the expected location of the fiducial markers. In patients treated with compression, the reference position was the location of the fiducial markers on the free-breathing planning CT. In patients treated with gating, the reference was the fiducial marker location on the 30% phase of the 4DCT. This difference is due to the fact that the real-time kV images are acquired at the beginning of the gating window (which is during the 30% phase). An expansion margin of 3 mm was added to all reference fiducial contours, which provides a 3 mm tolerance on the expected fiducial marker location.

Real-time target tracking was used to continuously verify patient alignment during treatment. This was accomplished using the Triggered Imaging capabilities of the Varian TrueBeam accelerator, which are described below. During MV treatment delivery, the system acquired kV planar images orthogonal to the treatment beam, and projected the contours of the fiducial markers onto the acquired images based on the angle of image acquisition. For each patient, the frequency and timing of image acquisition depended on the motion management strategy used. For abdominal compression, real-time kV images were taken every 20 degrees of the VMAT delivery. For gating, the kV images were acquired at the start of every gated 'beam-on' cycle. In both gating and compression, the time between real-time kV image acquisitions was approximately 5–6 seconds.

Two example real-time kV images are shown in Figure 1. The therapists were instructed to compare the fiducial marker locations in the acquired images against the reference fiducial contours. We prepared guidance materials and provided hands-on training to the therapists in order to accomplish this. If any of the markers were outside of the contours in 3 consecutive images, treatment was paused and adjustments were made. The nature of these adjustments are described below.

C. Impact of real-time tracking

Real-time imaging interventions were intended to correct two major categories of error. The first category was factors that caused radiation to be delivered to the wrong place, such as patient motion, tumor displacement, or significant digestive/bowel motion affecting tumor position. In these cases, shifts were necessary to re-localize the target. The other category of errors, such as erratic breathing or baseline drift of the respiratory trace, caused radiation to be delivered at the wrong time. In the case of downward drift of the respiratory trace (which represents the position of the Varian RPM infrared marker block on the patient's chest), the gating window becomes wider, and the beam turns on when the fiducial markers are inferior to their expected locations (vice versa in the case of upward drift) (29). If the fiducial markers were >3mm from the reference location in 3 consecutive images, treatment was halted. In cases where the patient's breathing trace exhibited baseline drift, the amplitude gating threshold was adjusted. Otherwise, the last acquired real-time kV image was used to re-align the fiducial markers to the reference location. Based on the angle at which the real-time kV image was acquired, the system translated this 2D image shift into a 3D couch shift. Note that, because images were acquired orthogonal to the treatment beam, errors in the direction of the treatment beam could not be detected or accounted for until later in the gantry rotation.

To characterize the effect of the real-time imaging system we quantified real-time treatment pauses. A real-time treatment pause (referred to as 'treatment pause' throughout the manuscript) was defined as any stop during treatment to either re-align the patient or to adjust the gating thresholds. In addition to number of treatment pauses, we characterized the magnitude of realignment shifts based on real-time imaging. The magnitude of these shifts was characterized in the anterior-posterior (AP), superior-inferior (SI), and left-right (LR) directions, as well as radially (total 3-D distance). These data were retrieved from the Record-and-Verify system (Aria, Varian Medical Systems).

The number of treatment pauses and magnitude of shifts were analyzed as a function of clinical and patient factors including motion management technique (compression versus gating), treatment time (defined as the time required to deliver all treatment fields in a session with no pauses or re-alignment shifts), number of implanted fiducials, PTV volume, and body mass index (BMI). The significance of observed differences in pauses and shifts was analyzed using multi-way Analysis of Variance (ANOVA).

D. Dosimetric analysis of patient alignment

We implemented an artificial neural network-based dosimetric model based on prior clinical pancreatic SBRT plans (33). This model draws on an existing database of clinical plans to predict the 3D dose distribution in the vicinity of the target. For each voxel within 5 cm of the PTV, the model used anatomical and geometric considerations (including distance to the PTV, PTV volume, and SI in-slice/out-of-slice location) to predict the dose distribution. A full description of the model is given in the Supplemental Methods. In essence, the model reduces the 3D dose distribution in the vicinity of the tumor to a curve that estimates the relationship between distance to the PTV and dose falloff. These data are shown in Figure S1. The model was used to calculate the dosimetric impact of a given real-time imaging shift

by referencing the magnitude of the shift against these falloff curves (taking into account dose falloff in both the LR/AP and SI directions). The results of this analysis is an estimate of the minimum dose to the target during one fraction, assuming the entire fraction had been delivered at the uncorrected position.

To study the effect of both target margins and motion on dose, we simulated the dosimetric impact of motion observed in our study in scenarios where the PTV margins were varied from 0 mm to 5 mm. Our calculation assumes that a re-alignment shift whose magnitude is less than the value of the GTV-to-PTV margin will have no significant impact on dose to the GTV. Consider the case of a target with 5 mm margins; if this tumor experiences a shift of <5 mm, then dose will not be significantly impacted since the tumor still resides entirely within the PTV. Likewise, if there are zero PTV margins, any shift causes the tumor to experience the full dosimetric impact of that displacement.

III. RESULTS

For each patient we characterized the frequency of treatment pauses per fraction (pause rate). Data characterizing the number of treatment pauses is presented in Table 2. For the entire 68 patient cohort, the total number of treatment pauses was 268 which equates to an average of 3.9 treatment pauses per patient over the entire course of treatment and a pause rate of 0.81. 60% of the treatment pauses were due to having to adjust the gating thresholds and 40% were due to having to re-localize the target. The average time per pause was 1.9 1.8 minutes; 5% of pauses were longer than 5 minutes ± and 1% were longer than 10 minutes. There was no significant difference in time per pause for gating adjustments vs re-localization. The median treatment time was 8.1 min (range: 2.3 − 22.1 min). The pause rate was significantly higher in patients treated with gating ($p<0.001$) and for patients with greater treatment time ($p=0.01$). Figure 2 provides a box plot binning the pause rate according to treatments that are <200 seconds, 200 to 400 seconds, 400 to 600 seconds, and >600 seconds.

There were 107 treatment pauses (0.32 pauses per fraction) where patient re-alignment was triggered by the real-time target tracking system. A histogram of the shifts is shown in Figure 3. The median shifts for patient re-alignment were 0.8 mm (AP), 4.0 mm (SI), and 1.2 mm (LR). The median radial (3D) shift was 5.2 mm. 41% of all patients had at least one shift throughout the course of treatment with magnitude >5 mm, and 16% of all fractions had at least one treatment pause that required an alignment >5 mm. Table 2 characterizes the magnitude of shifts with respect to patient and clinical factors. The magnitude of shifts was significantly higher in patients with greater treatment time ($p=0.01$).

The dosimetric effect of real-time imaging shifts was calculated using the derived dosimetric model (see Supplementary Material), and cumulative histograms of these data are shown in Fig 4. The data are shown in a similar manner as a dose-volume histogram; each point represents the probability of observing a shift with dosimetric impact less than or equal to the value along the x-axis. The data are shown for different theoretical values of PTV margin. In the 5 mm (clinical) scenario, 45% of shifts resulted in point dose differences

averaging 23% ± 22% of the prescription dose. However, 55% of observed shifts resulted in no noticeable target dose difference (y-intercept of 55%).

IV. DISCUSSION

As more institutions explore ablative dose schedules in pancreatic SBRT, it is imperative to understand the potential risks and benefits. Motion is a first-order driver of uncertainty, and there is significant need to characterize the benefit of different motion mitigation techniques. In this study, we characterized the impact of real-time target tracking on our clinical workflow, the potential gains in treatment accuracy, and the potential dosimetric benefits in target coverage.

4DCT is the most widely-used technique for understanding tumor motion, yet studies have demonstrated that a single 4DCT is not a reliable predictor of motion for pancreas SBRT (10–13). As a result of the inconsistent organ and tumor motion, using fiducials along with real-time image guidance has taken on an increased role in performing pancreas SBRT. Data is needed to provide guidance on practical implementation of real-time target tracking for abdominal SBRT treatments. We provide the first report, of a large, 68 patient cohort experience for patients treated with real-time target tracking on a conventional linear accelerator. The data presented in the current work characterizes the frequency of treatment pauses needed to re-optimize patient set-up, the magnitude of shifts required when re-alignment is necessary, and the dosimetric impact of the real-time target tracking system.

Our pancreatic SBRT patients monitored with real-time target tracking experienced treatment pauses (either due to patient re-alignment or a gating threshold adjustment) at an average rate of 0.80 per fraction. In other words, treatment will have to be paused approximately four times every five fractions for each patient monitored with real-time target tracking. About 60% of the time, the treatment pauses were due to needing to adjust amplitude gating thresholds due to baseline drift of the respiratory trace and 40% were due to needing to re-align the patient. Since there is no need to adjust thresholds during treatment with compression, the number of treatment pauses required was significantly higher in patients treated with gating. We believe there are two possible reasons for the increase in pause rate as a function of treatment time, either 1) the probability of pauses is constant, and so longer treatment time translates to more pauses, or 2) the longer the patient remains on the table, the more likely their position and breathing will deviate from the initial setup. The dependence of treatment pauses on treatment time that our data presents is in line with previous work which demonstrated that the agreement between pre-treatment tumor motion measured with 4DCT and post-treatment tumor motion significantly decreases for treatments times > 7.5 minutes. (13).

Our data showed that real-time target tracking triggered a patient re-alignment event at a rate of 0.32 shifts per fraction. The re-alignment data presented in our study can be compared to previous work using similar real-time kV imaging technology to monitor prostate (18,19), and abdominal treatments (20, 21). Worm et al (21) reported SI shifts of > 3mm for 39.2% of all fractions and shifts > 5 mm for 11.3% of all fractions for 10 liver SBRT patients. Yorke et al (20) report SI displacements of > 5 mm for 7.6% of all fractions for 19

abdominal SBRT patients treated with compression. Keall et al (18) report a 'gating event' (using a 3-mm/5-second criteria) for 14.5% of all fractions (19) for 6 prostate patients. The lower shift rates reported by Keall et al (19) are expected given that the prostate is thought to be a more stable target when compared to lesions treated in the abdomen. The shifts reported by Worm et al and Yorke et al (20) for liver SBRT patients are in line with our realignment rates of 45% and our > 5 mm re-alignments for 14% of all fractions. The rate of patient re-alignment needed during treatment can be explained by the variability of tumor motion for abdominal SBRT treatments reported previously (12, 34, 35).

We found that making corrections to the tumor position based on real-time target tracking resulted in dosimetric benefits. We utilized a neural network-based dosimetric model to predict dose falloff in the tumor vicinity, and calculated the effect of tumor re-alignment on dose to the edges of the tumor. Based on dosimetric simulations (Fig. 4), 45% of shifts resulted in target coverage benefits; however, 55% of observed shifts resulted in no noticeable target dose difference. This result could potentially be interpreted two ways: either the fiducial distance criteria (3 mm) could be relaxed (and thereby reducing the frequency of shifts), or the treatment margins (5 mm) could be made smaller. In the hypothetical 2 mm scenario presented in Fig. 4, all shifts had clinical impact (y-intercept = 0), and the data suggest that no dosimetrically beneficial shifts were missed (x-intercept =0). Further study is warranted to understand the interplay between these factors and to explore the potential for real-time imaging interventions to enable safe margin reduction or dose escalation.

It should be noted that our model does not account for several clinically relevant factors, and should be considered in context. Our model, in essence, calculates a standardized 3D dose distribution based on prior clinical data. The benefit of this approach is that the dosimetric impact of real-time imaging shifts can be computed using data for an "average" patient plan (and are not overly biased by shifts in a single patient whose plan may be more sensitive to motion). The model calculates changes in point dose at the edge of the tumor volume, normalized as a fraction of prescription dose. The true effect of this shift depends on how early in treatment the shift occurred, and how much dose would have been delivered in the absence of a corrective shift. In that sense, the point dose values presented by our model represent a worst-case scenario for decreases in minimum tumor dose due to target motion. Also, the effect is estimated for a single fraction, and it is possible that these errors would be averaged out by dose given during other fractions. It should also be noted that the model does not include dose to normal structures, and so many of the shifts that did not result in target dose changes may have resulted in significant changes to normal tissue dose (e.g. the duodenum). Knowledge of the changes in dose to normal tissue may impact the interpretation of Figure 4, and we feel that further study is warranted to understand the full dosimetric impact of real-time imaging shifts in pancreatic SBRT.

The procedure described in this work relies on the accuracy of fiducial markers as surrogates for tumor position, and errors could occur in the presence of tumor deformation or marker migration. Feng et al characterized the challenges in establishing reliable surrogates for pancreatic tumor position (15), and noted that deformation of pancreatic tumor borders does occur. However, we argue that the average size of these deformations is relatively small (1–2

mm) compared to the other uncertainties present during pancreatic SBRT (such as motion). Studies by Choi et al and Sanders et al noted a spontaneous fidicial migration rate of 3–7% (36, 37), which agrees qualitatively with our experience. Clinically, we find that in cases with three or more fiducial markers, it is feasible to detect when one has migrated by comparing the relative positions of the markers to one another and looking for outliers. For this reason, we argue that it is critical to implant at least three markers for pancreatic SBRT (with four being the preferred number in case one marker migrates significantly before simulation).

V. CONCLUSIONS

In this study, we quantified the benefit of fiducial-based real-time target tracking to increase the accuracy of pancreatic SBRT. This dataset represents, to our knowledge, the largest experience treating these tumors with fiducial marker-guided in-treatment kV imaging. We found that, following initial alignment with CBCT, patients needed to be re-aligned in roughly 32% of treated fractions. Our data demonstrated that applying these re-alignment shifts resulted in dosimetric benefits via increased tumor coverage. The real-time target tracking workflow introduced practical hurdles into day-to-day operations, but there were no significant issues that hindered treatment.

Supplementary Material

Refer to Web version on PubMed Central for supplementary material.

ACKNOWLEDGEMENTS

This work was funded in part by the National Institutes of Health under award number K12CA086913, the University of Colorado Cancer Center/ACS IRG #57-001-53 from the American Cancer Society, the Boettcher Foundation, and Varian Medical Systems. These funding sources had no involvement in the study design; in the collection, analysis and interpretation of data; in the writing of the manuscript; or in the decision to submit the manuscript for publication.

VII. CONFLICT OF INTEREST

Dr. Jones and Dr. Miften report grants from Varian Medical Systems, during the conduct of the study; in addition, Dr. Jones and Dr. Miften have a patent Automated Tracking of Fiducial Marker Clusters in X-Ray Images, US Provisional Patent Application 62/368,870 pending.

REFERENCES

[1]. Koong AC, Le QT, Ho A, et al. Phase I study of stereotactic radiosurgery in patients with locally advanced pancreatic cancer. Int J Radiat Oncol 2004;58:1017–1021.

[2]. Chuong MD, Springett GM, Freilich JM, et al. Stereotactic body radiation therapy for locally advanced and borderline resectable pancreatic cancer is effective and well tolerated. Int J Radiat Oncol 2013;86:516–522.

[3]. Brunner TB, Nestle U, Grosu A-L, et al. SBRT in pancreatic cancer: What is the therapeutic window? Radiother Oncol 2015;114:109–116. [PubMed: 25466369]

[4]. Hoyer M, Roed H, Sengelov L, et al. Phase-II study on stereotactic radiotherapy of locally advanced pancreatic carcinoma. Radiother Oncol 2005;76:48–53. [PubMed: 15990186]

[5]. Mori S, Hara R, Yanagi T, et al. Four-dimensional measurement of intrafractional respiratory motion of pancreatic tumors using a 256 multi-slice CT scanner. Radiother Oncol 2009;92:231–237. [PubMed: 19211167]

[6]. Xi M, Liu M-Z, Deng X-W, et al. Defining internal target volume (ITV) for hepatocellular carcinoma using four-dimensional CT. Radiother Oncol 2007;84:272–278. [PubMed: 17727988]

[7]. Xi M, Liu M-Z, Zhang L, et al. How many sets of 4DCT images are sufficient to determine internal target volume for liver radiotherapy? Radiother Oncol 2009;92:255–259. [PubMed: 19520447]

[8]. Cattaneo GM, Passoni P, Sangalli G, et al. Internal target volume defined by contrast-enhanced 4D-CT scan in unresectable pancreatic tumour: evaluation and reproducibility. Radiother Oncol 2010;97:525–529. [PubMed: 20826027]

[9]. Heinzerling JH, Anderson JF, Papiez L, et al. Four-dimensional computed tomography scan analysis of tumor and organ motion at varying levels of abdominal compression during stereotactic treatment of lung and liver. Int J Radiat Oncol 2008;70:1571–1578.

[10]. Yang W, Fraass BA, Reznik R, et al. Adequacy of inhale/exhale breathhold CT based ITV margins and image-guided registration for free-breathing pancreas and liver SBRT. Radiat Oncol 2014;9:11. [PubMed: 24401365]

[11]. Ge J, Santanam L, Noel C, et al. Planning 4-dimensional computed tomography (4DCT) cannot adequately represent daily intrafractional motion of abdominal tumors. Int J Radiat Oncol 2013;85:999–1005.

[12]. Lens E, van der Horst A, Kroon PS, et al. Differences in respiratory-induced pancreatic tumor motion between 4D treatment planning CT and daily cone beam CT, measured using intratumoral fiducials. Acta Oncol 2014;53:1257–1264. [PubMed: 24758251]

[13]. Rankine L, Wan H, Parikh P, et al. Cone-beam computed tomography internal motion tracking should be used to validate 4-dimensional computed tomography for abdominal radiation therapy patients. Int J Radiat Oncol 2016;95:818–826.

[14]. Jones BL, Schefter T, Miften M. Adaptive motion mapping in pancreatic SBRT patients using Fourier transforms. Radiother Oncol 2015;115:217–222. [PubMed: 25890573]

[15]. Feng M, Balter JM, Normolle D, et al. Characterization of pancreatic tumor motion using cine MRI: surrogates for tumor position should be used with caution. Int J Radiat Oncol 2009;74:884–891.

[16]. Méndez Romero A, Wunderink W, Hussain SM, et al. Stereotactic body radiation therapy for primary and metastatic liver tumors: a single institution phase i-ii study. Acta Oncol 2006;45:831–837. [PubMed: 16982547]

[17]. Pishvaian AC, Collins B, Gagnon G, et al. EUS-guided fiducial placement for CyberKnife radiotherapy of mediastinal and abdominal malignancies. Gastrointest Endosc 2006;64:412–417. [PubMed: 16923491]

[18]. Keall PJ, Aun Ng J, O'Brien R, et al. The first clinical treatment with kilovoltage intrafraction monitoring (KIM): A real-time image guidance method. Med Phys 2015;42:354–358. [PubMed: 25563275]

[19]. Keall PJ, Ng JA, Juneja P, et al. Real-time 3D image guidance using a standard LINAC: measured motion, accuracy, and precision of the first prospective clinical trial of kilo-voltage intrafraction monitoring–guided gating for prostate cancer radiation therapy. Int J Radiat Oncol 2016;94:1015–1021.

[20]. Yorke E, Xiong Y, Han Q, et al. Kilovoltage Imaging of Implanted Fiducials to Monitor Intrafraction Motion With Abdominal Compression During Stereotactic Body Radiation Therapy for Gastrointestinal Tumors. Int J Radiat Oncol 2016;95:1042–1049.

[21]. Worm ES, Høyer M, Fledelius W, et al. Three-dimensional, time-resolved, intrafraction motion monitoring throughout stereotactic liver radiation therapy on a conventional linear accelerator. Int J Radiat Oncol 2013;86:190–197.

[22]. Wurm RE, Gum F, Erbel S, et al. Image guided respiratory gated hypofractionated Stereotactic Body Radiation Therapy (H-SBRT) for liver and lung tumors: Initial experience. Acta Oncol 2006;45:881–889. [PubMed: 16982554]

[23]. Wang B, Rassiah-Szegedi P, Huang HZ, et al. Initial experience and clinical comparison of two image guidance methods for SBRT treatment: 4DCT versus respiratory-triggered imaging. J Appl Clin Med Phys 2011;12:257–267.

[24]. Kupelian PA, Willoughby TR, Meeks SL, et al. Intraprostatic fiducials for localization of the prostate gland: monitoring intermarker distances during radiation therapy to test for marker stability. Int J Radiat Oncol 2005;62:1291–1296.

[25]. Seppenwoolde Y, Berbeco RI, Nishioka S, et al. Accuracy of tumor motion compensation algorithm from a robotic respiratory tracking system: a simulation study. Med Phys 2007;34:2774–2784. [PubMed: 17821984]

[26]. Zhang H, Zhao G, Djajaputra D, et al. Determination of acquisition frequency for intrafractional motion of pancreas in CyberKnife radiotherapy. textitSci World J 2014.

[27]. Zhang P, Goodman K, Han Q, et al. Setting Action Levels for Abdominal Stereotactic Body Radiation Therapy Monitored With Frequent kV Imaging Surveillance. Int J Radiat Oncol 2014;90:S828.

[28]. Santoro JP, Yorke E, Goodman KA, et al. From phase-based to displacement-based gating: a software tool to facilitate respiration-gated radiation treatment. J Appl Clin Med Phys 2009;10:132–141.

[29]. Mageras GS, Yorke E. Deep inspiration breath hold and respiratory gating strategies for reducing organ motion in radiation treatment. Semin Radiat Oncol 2004;14:65–75. [PubMed: 14752734]

[30]. Berbeco RI, Nishioka S, Shirato H, et al. Residual motion of lung tumours in gated radiotherapy with external respiratory surrogates. Phys Med Biol 2005;50:3655. [PubMed: 16077219]

[31]. Fuji H, Asada Y, Numano M, et al. Residual motion and duty time in respiratory gating radiotherapy using individualized or population-based windows. Int J Radiat Oncol 2009;75:564–570.

[32]. Campbell WG, Jones BL, Schefter T, et al. An evaluation of motion mitigation techniques for pancreatic SBRT. Radiother Oncol 2017.

[33]. Campbell WG, Miften M, Olsen L, et al. Neural network dose models for knowledge-based planning in pancreatic SBRT. Med Phys 2017;44:6148–6158. [PubMed: 28994459]

[34]. Ge J, Santanam L, Yang D, et al. Accuracy and consistency of respiratory gating in abdominal cancer patients. Int J Radiat Oncol 2013;85:854–861.

[35]. Jayachandran P, Minn AY, Van Dam J, et al. Interfractional uncertainty in the treatment of pancreatic cancer with radiation. Int J Radiat Oncol 2010;76:603–607.

[36]. Choi J-H, Seo D-W, Do Hyun Park SKL, et al. Fiducial placement for stereotactic body radiation therapy under only endoscopic ultrasonography guidance in pancreatic and hepatic malignancy: practical feasibility and safety. Gut Liver 2014;8:88. [PubMed: 24516706]

[37]. Sanders MK, Moser AJ, Khalid A, et al. EUS-guided fiducial placement for stereotactic body radiotherapy in locally advanced and recurrent pancreatic cancer. Gastrointest Endosc 2010;71:1178–1184. [PubMed: 20362284]

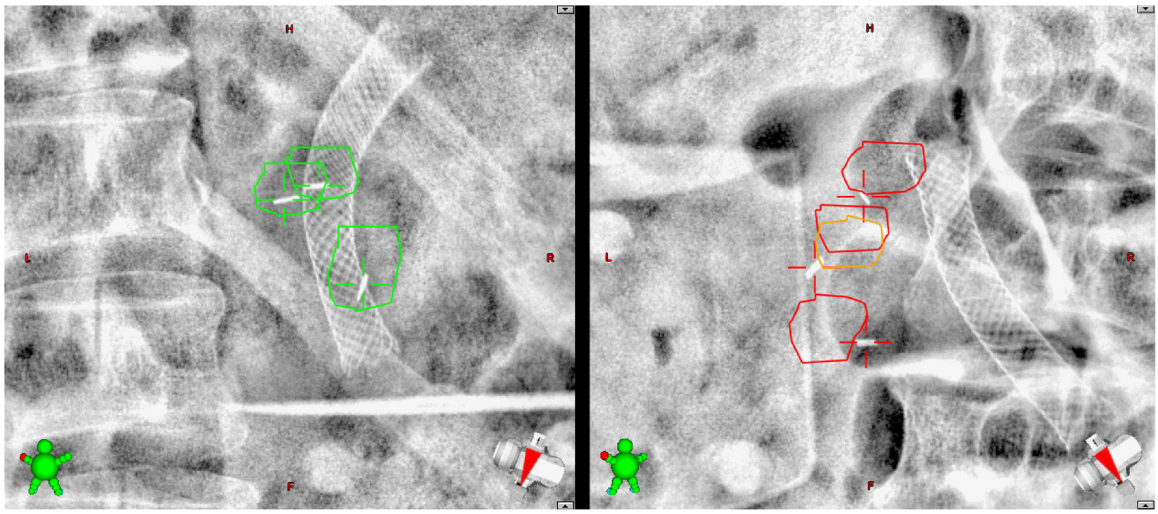

FIG. 1.

Clinical real-time kV images. The expected fiducial marker locations (plus 3 mm margin) were projected onto the kV images acquired during treatment (orthogonal to the treatment beam). On the left, the markers are within the expected region, and treatment was allowed to proceed. On the right, the markers were outside of the expected area, and treatment was halted. The spinal column, ribs, abdominal gas, and biliary stents are also visible in these images.

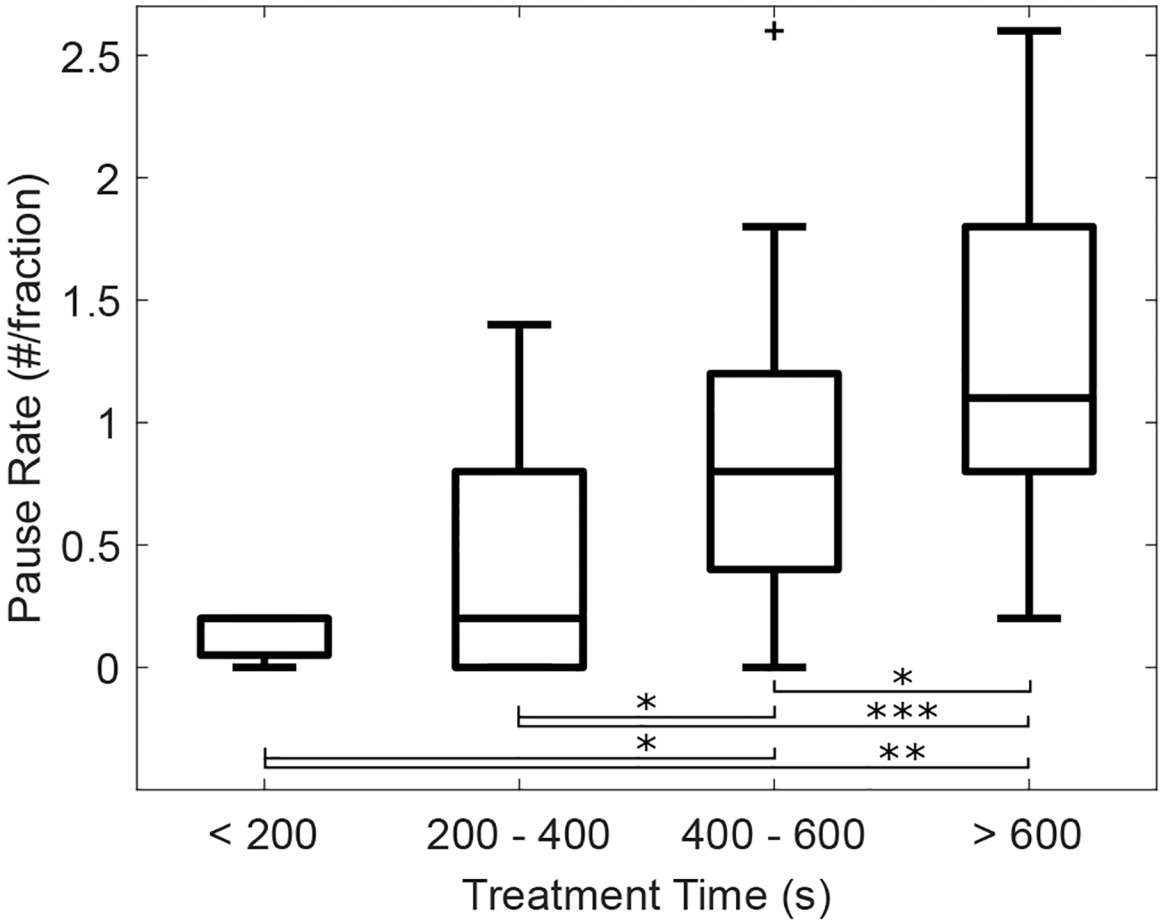

FIG. 2.

Relationship between the number of pauses per treatment fraction (pause rate) and treatment time. The number of treatment pauses per fraction is significantly higher as the treatment time increases. In these box plots, the upper and lower lines represent the range of the data, the inner box gives the 25th–75th percentile, and the middle line denotes the median. P-value thresholds of <0.05, <0.01, and <0.001 are denoted by *, **, and ***, respectively.

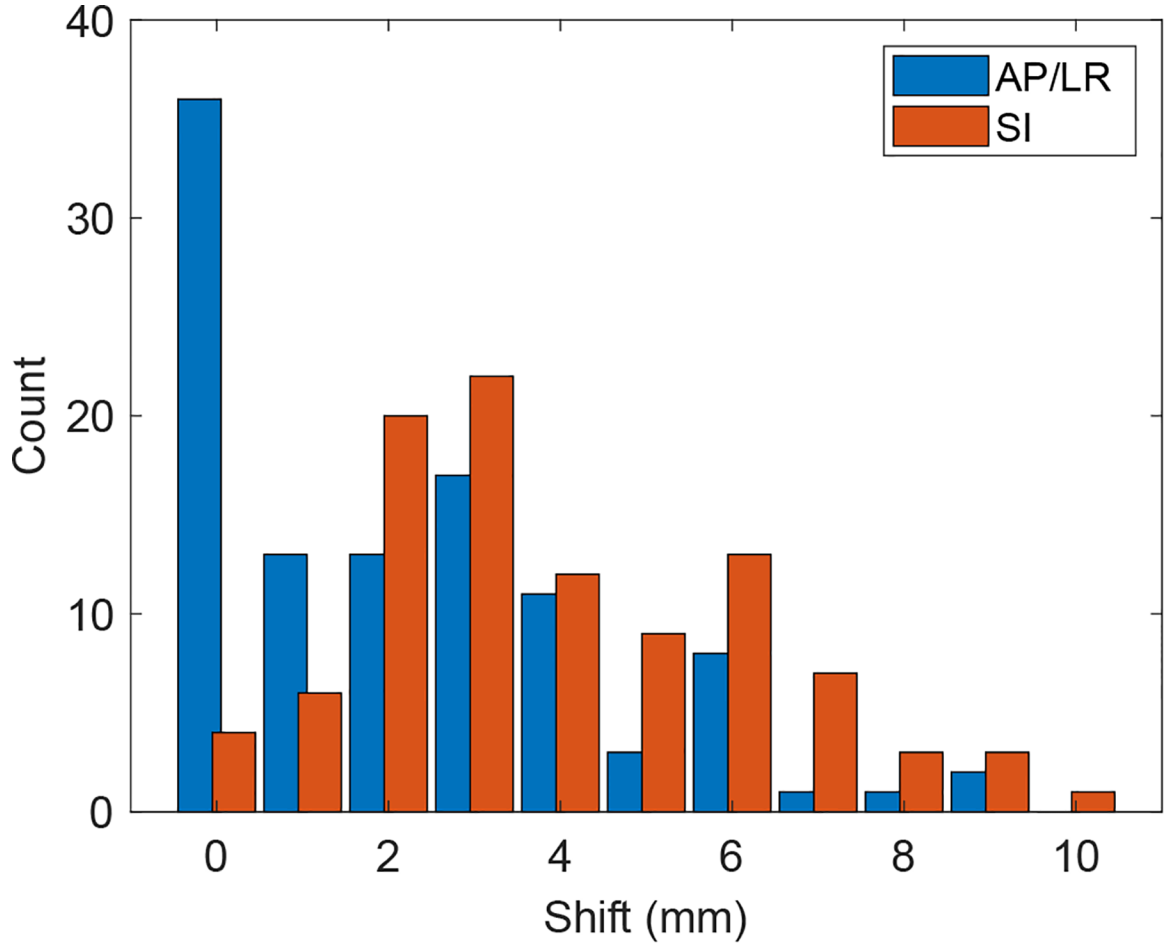

FIG. 3.

Histogram of the distance of shifts triggered by the real-time tumor tracking system. Values are shown in the in-plane (AP/LR) and SI directions. The average radial shift was 5.9 mm, and the primary component of these shifts was in the SI direction.

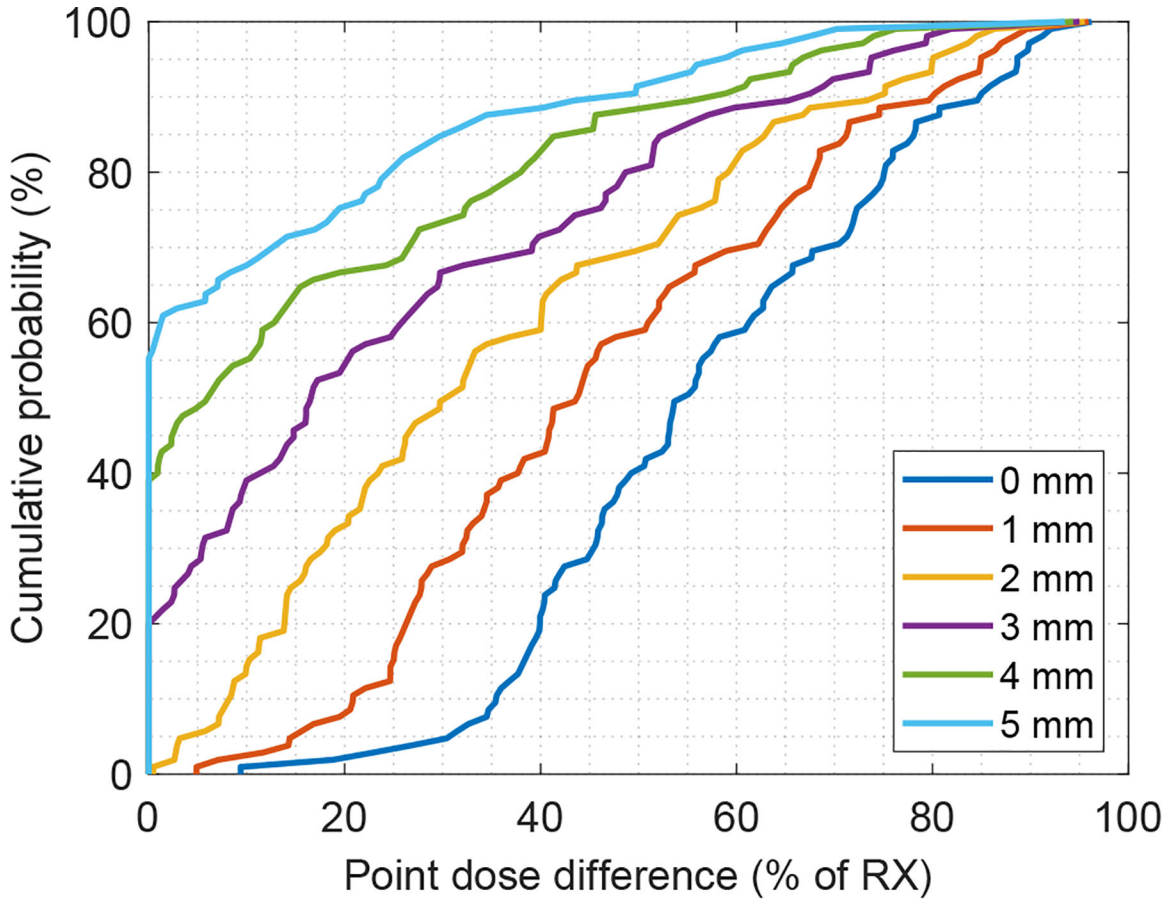

FIG. 4.

Cumulative histogram of the dosimetric effect of real-time imaging shifts. The dosimetric effect was estimated using the artificial neural network dosimetric model, and was calculated for PTV margins ranging from 0 – 5 mm. The data are shown in a similar manner as a dose-volume histogram; each point represents the probability of observing a shift with dosimetric impact less than or equal to the value along the x-axis (displayed as a percentage of the prescription dose). For instance, in the 5 mm margin scenario, 55.5% of the observed shifts resulted in no significant point-dose differences (y-intercept of 55.5%). In the 0 mm margin scenario, each shift resulted in a point dose difference of at least 10% (x-intercept of 10%).

TABLE I.

Clinical, treatment, and motion management parameters of the pancreatic SBRT study cohort. BMI = Body Mass Index, PTV = Planning Target Volume

Cohort	**Number**	
All Patients	68	
Gating	53 (78%)	
Compression	15 (22%)	
	Median	**Range**
Dose per Fraction	660 cGy	500 – 900 cGy
Number of Fractions	5	3 – 5
Number of Fiducials	3	1 – 7
Treatment Time	485 s	137 – 1331 s
PTV Volume	41 cm^3	16 – 349 cm^3
BMI	23	17 – 40

TABLE II.

Characterization of real-time treatment pauses per fraction (pause rate) and magnitude of shifts required for patient re-alignment. A treatment pause was defined as any stop during treatment to either re-align the patient (triggered by the real time tumor tracking system) or to adjust the gating thresholds. The means were compared using ANOVA. BMI = Body Mass Index, PTV = Planning Target Volume

Cohort	Treatment Pauses (#/fx)		Re-alignment shifts (mm)		
	Pause Rate	*p*	Median	StDev	*p*
All Patients	0.81		5.2	2.9	
Technique		<0.001			0.65
Gating	1.00		5.3	2.8	
Compression	0.16		3.6	3.4	
Number of Fiducials		0.60			0.28
<3	0.87		5.8	3.8	
≥3	0.78		4.8	2.6	
Treatment Time		0.01			0.01
< 485 s	0.57		4.7	1.9	
≥ 485 s	1.06		5.3	3.2	
PTV Volume		0.65			0.26
< 41 cm^3	0.84		5.3	2.8	
≥ 41 cm^3	0.80		5.1	2.9	
BMI		0.85			0.60
< 23	0.83		5.2	3.3	
≥ 23	0.82		5.3	2.3	

Int J Radiat Oncol Biol Phys. Author manuscript; available in PMC 2019 June 27.